Charge State Dependent Energy Loss of Slow Ions - Part A: Experimental Results on Highly Charged Ion Transmission

Richard A. Wilhelm,[1,*] Elisabeth Gruber,[2] Valerie Smejkal,[2] Stefan Facsko,[1] and Friedrich Aumayr[2]

[1] *Helmholtz-Zentrum Dresden-Rossendorf, Institute of Ion Beam Physics and Materials Research, 01328 Dresden, Germany, EU*
[2] *TU Wien, Institute of Applied Physics, 1040 Vienna, Austria, EU*

(Dated: October 29, 2015)

We report on energy loss measurements of slow ($v \ll v_0$) highly charged ($Q > 10$) ions upon transmission through a 1 nm thick carbon nanomembrane. We emphasize here the scaling of the energy loss with velocity and charge exchange/loss. We show that a weak linear velocity dependence exists, whereas charge exchange dominates the kinetic energy loss especially in the case of large charge capture. A universal scaling of the energy loss with charge exchange and velocity is found and discussed in this paper. A model for charge state dependent energy loss for slow ions is presented in part B of this series [Wilhelm, R.A., Möller, W., Phys. Rev. A., submitted (2015)].

PACS numbers: 34.35.+a, 34.50.Bw, 34.70.+e, 68.49.Sf, 68.65.-k, 79.20.Rf
Keywords: low energy ions, ion charge state, stopping power, energy loss, highly charged ion, charge exchange

I. INTRODUCTION

How ions dissipate their energy when moving through matter was of interest since the early years of the last century [1]. Ions impacting on a solid surface may lose kinetic energy (or in the case of highly charged ions also potential energy) as a result of collisions with target electrons and nuclei [2–6].

A corresponding distinction into electronic and nuclear energy loss (so called 'stopping') is usually made but not necessarily justified, since the individual processes involved might be coupled [5, 6]. First order perturbation approaches predict a dependence of the energy loss with the square of the projectile's nuclear charge Z_1 but are only valid at sufficiently high projectile velocities v. Such approaches are however inadequate for a heavy ion at low impact velocities [7], where charge exchange, excitation and ionization processes (involving electrons from the target but also from the projectile) alter the ion's charge state until a dynamic charge and excitation state equilibrium of the projectile is reached [8, and ref. therein] [9–13]. Of course the screening of the Coulomb potential of the nuclear charge by the captured electrons affects the stopping force. This is sometimes taken into account by using an effective charge, a concept that has been pointed out to be somewhat misleading [7] and at most empirically justified.

Of particular interest in this connection is the charge state dependence of energy loss and in particular preequilibrium effects, like e.g. the energy loss of projectile ions, which have not yet reached their equilibrium charge state. At velocities $v < v_0$ (with v_0 being the Bohr velocity) the equilibrium charge is typically very small ($Q_{eq} \approx Z^{1/3} v/v_0 \leq 2$ [14]). Preequilibrum phenomena are therefore best studied with slow highly charged ions, whose charge state is far from equilibrium ($10 \leq Q \leq Z_1$). Since corresponding equilibration lengths in solids are quite small (at most a few nm [9, 11, 15, 16]), ultrathin target films are desirable to minimize the projectiles trajectory in the solid. Information on the equilibration and energy loss dynamics can be important for applications, like e.g. nanostructuring of surfaces by slow highly charged ions, since it allows to estimate the depth below the surface where the projectiles' potential energy can still be deposited [17–19].

Part A of this series of two papers presents experimental results on the energy loss (stopping) of slow ($v \ll v_0$) highly charged Xe ions transmitted through a 1 nm thin carbon nanomembrane. We will discuss the dependence of energy loss on incident and exit charge state as well as impact velocity and present an empirical scaling consolidating our findings. In Part B of this series [20] model for a charge state dependent energy loss of slow ions is elaborated and compared with the experimental data.

II. EXPERIMENTAL SETUP

Highly charged ions are produced in a room-temperature electron beam ion trap (EBIT) from Dreebit GmbH, Germany. The base pressure in the ion source is 10^{-10} mbar and during operation a pressure of 3×10^{-9} mbar is maintained by introducing isotope pure ^{129}Xe gas. A DC ion current is extracted in the leaky mode of the EBIT at a kinetic energy of 4.4 keV$\times Q$ (Q denotes the ion charge state). An analyzing magnet is utilized to charge state separate the extracted ion beam which is then focused into a target chamber by several electrostatic lens assemblies. The ion source and beamline are negatively biased with respect to the target chamber which allows us to decelerate the ion beam when it enters the target chamber at ground potential. (Note, that the ion source is biased at +4.4 kV with respect to the beamline.) A final electrostatic lens assembly, the deceleration lens,

* Author to whom correspondence should be addressed. Electronic mail: r.wilhelm@hzdr.de

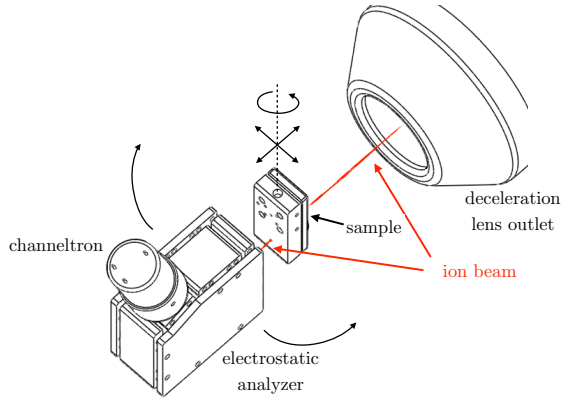

FIG. 1. (color online) Sketch of the ion beam passing through the sample holder into the electrostatic analyzer. The analyzer can be rotated around the sample.

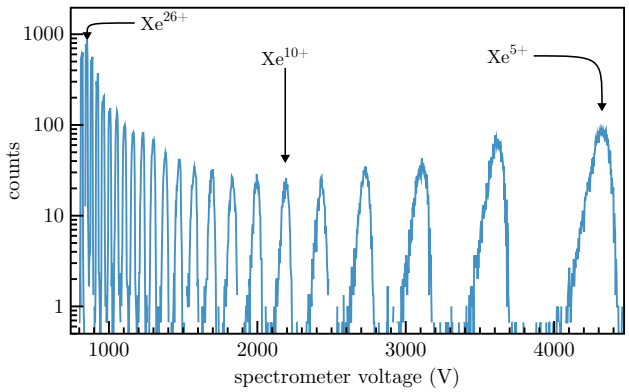

FIG. 2. (color online) Exit charge state spectrum of Xe^{28+} ions at $E_{kin} = 126\,\text{keV}$ transmitted through a 1 nm thick carbon nanomembrane. The spectrum is bimodal.

reachtes into the chamber to reduce the field free flight pass as much as possible. Even at lowest (final) kinetic energies of 4 keV a beam spot size of around 1 mm in diameter can be maintained. The target chamber is kept at ultrahigh vacuum conditions (10^{-9} mbar) during measurements. An electrostatic analyzer with a relativ energy resolution of $\Delta E/E \approx 1.5 \times 10^{-3}$ is mounted in the target chamber and allows energy and charge state separation of the ions after transmission through thin samples. The analyzer can be rotated around the sample axis in order to perform angle resolved transmission measurements. Ions are counted in a Hamamatsu Photonics channeltron after passing through the analyzer. Fig. 1 shows a sketch of the sample-analyzer arrangement in the chamber with the respective axes of movement for the sample and analyzer.

Samples are produced by CNM Technologies Bielefeld, Germany by cross-linking a self-assembled monolayer of biphenyl-4-thiol molecules on a Au substrate with low energy electrons [21]. The cross-linked monolayer is released from the substrate by chemical etching and transferred to a standard transmission electron microscopy (TEM)-grid with a thick lacey-carbon support. A load-lock is used to bring the TEM-grid into the target chamber without breaking vacuum in the chamber or beamline.

Before the actual transmission experiments, the energy and charge state distribution of the ion beam were checked without sample. The incident kinetic energy E_0 has a width of $\Delta E_0 \approx 10^{-3} E_0$ and is thus smaller than the measurement resolution. Small charge exchange with $Q \to Q-1$ in order of 10^{-3} was observed due to scattering with rest gas atoms in the approximately 5 m long beamline. Since the charge exchange discussed here is 1 to 2 orders of magnitude more intense combined with much larger ΔQ, we regard the incoming beam as prepared exclusively in the desired charge state Q.

III. MEASUREMENTS

The ion transmission of highly charged xenon through the described carbon nanomembranes results in a spectrum of exit charge states. The spectrum is twofold as depicted in fig. 2 and discussed already in [22]. The energy loss, however, is dependent on the exit charge state Q_{exit} (or in other words on the charge exchange $\Delta Q = Q_{in} - Q_{exit}$). Additionally, electronic stopping is considered to scale linearly with the ion velocity for slow ions [4, 23]. We measured the velocity dependence of the energy loss and the results are shown in fig. 3 for Xe^{20+} ions. The energy loss increases linearly with velocity between 1.5×10^5 m/s and 2.5×10^5 m/s for the lower exit charge states ($Q_{exit} \leq 5$). For larger exit charge states, i.e. smaller charge exchange the dependence on the ion velocity gets smaller and almost vanishes. At an even higher velocity of 3.6×10^5 m/s the energy loss decreases, thus the linear velocity scaling is not entirely preserved the in case of highly charged ions [24]. Fig. 3 already shows that the energy loss depends on more than one parameter in a complex way.

Fig. 4 shows the energy loss as a function of the exit charge state Q_{exit} or charge loss $\Delta Q = Q_{in} - Q_{exit}$ for different ion velocities ranging from 1.8×10^5 m/s ($0.08 v_0$) to 3.7×10^5 m/s ($0.17 v_0$). Here a common dependence on the charge exchange can already be seen. The energy loss is strongly dependent on the charge exchange, but also on the incident charge state and/or velocity. However, the velocity dependence is small

A quadratic dependence of the energy loss on the incident charge state is commonly assumed in literature [25] and was recently measured in experiment [22]. Fig. 5 shows the incident charge state dependence of the energy loss for a fixed ion velocity and different exit charge states (charge exchange). Here, the quadratic dependence can be seen as well (dotted-dashed line for $Q_{exit} = 2$). The data points are also fitted with a function $\Delta E = \alpha + \beta Q_{in} e^{\gamma (Q_{in} - Q_{exit})/Q_{in}}$, which results from

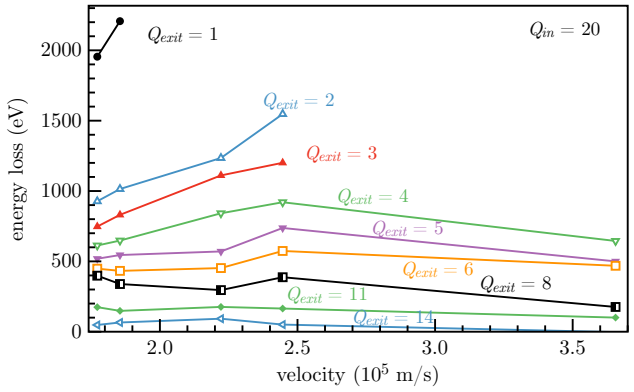

FIG. 3. (color online) Energy loss of Xe^{20+} transmitted through a 1 nm thick carbon nanomembrane as a function of ion velocity for different observed charge exchanges (exit charge states). For large charge exchange and velocities around 2×10^5 m/s the energy loss scales linearly with velocity, whereas it becomes independent on the velocity for smaller charge exchange. For a higher velocity of about 3.6×10^5 m/s the energy loss decreases.

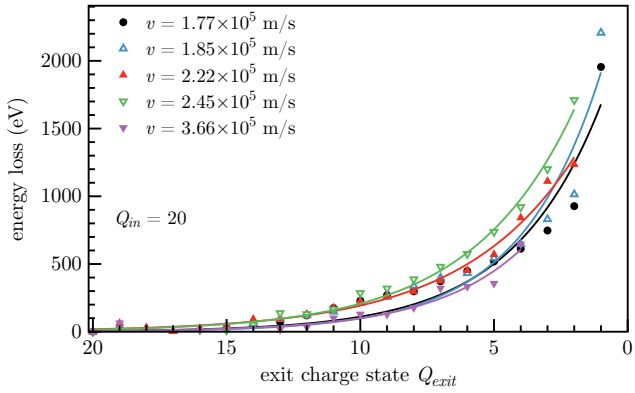

FIG. 4. (color online) Energy loss as a function of exit charge state for different ion velocities v and $Q_{in} = 20$. The target material is again a 1 nm thick carbon nanomembrane. The data is fitted by a function $\alpha e^{\beta(Q_{in}-Q_{exit})/Q_{in}}$ (see text).

a universal scaling of our results with charge exchange (see below). The quadratic fit and the universal scaling fit the data in fig. 5 equally well. The parameters α, β and γ range from 50-240 eV, $2\times10^{-4} - 0.5$ eV, and 8-14, respectively. Note that the exponent ranges only from 0 to γ ($\Delta Q/Q_{in} \leq 1$).

Summarizing, we see a weak dependence of the energy loss on ion velocity (fig. 3), a strong dependence on charge loss/exchange (fig. 4) and a quadratic dependence on the incident charge state (fig. 5).

To find a universal scaling of the energy loss, ions at different incident charge states from $Q_{in} = 10$ to 42 were used at different kinetic energies of 4400 eV$\times Q_{in}$ (44 keV to 185 keV), i.e. different ion velocities. The energy loss was measured for each exit charge state, thus all three

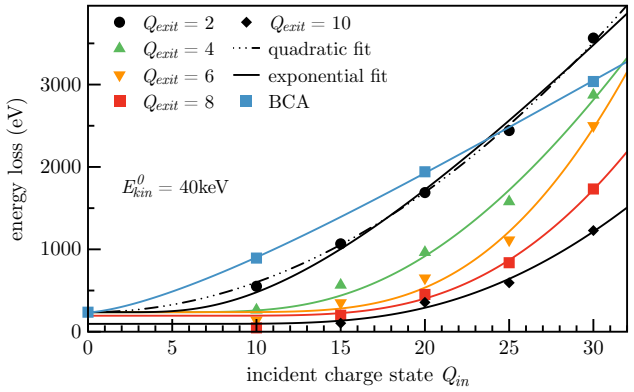

FIG. 5. (color online) Energy loss of Xe ions transmitted through a 1 nm thick carbon nanomembrane as function of the incident charge state for different charge exchanges (exit charge states). The primary kinetic energy is here fixed to 40 keV. The energy loss was fitted with a function $\Delta E = \alpha + \beta Q_{in} e^{\gamma(Q_{in}-Q_{exit})/Q_{in}}$ (see text). To compare for the $Q_{exit} = 2$ data, a quadratic fit is shown as well as suggested recently in [22]. Additionally a result from a binary collision approximation (BCA) simulation is shown as blue squares. The simulation is explained in detail in [20]

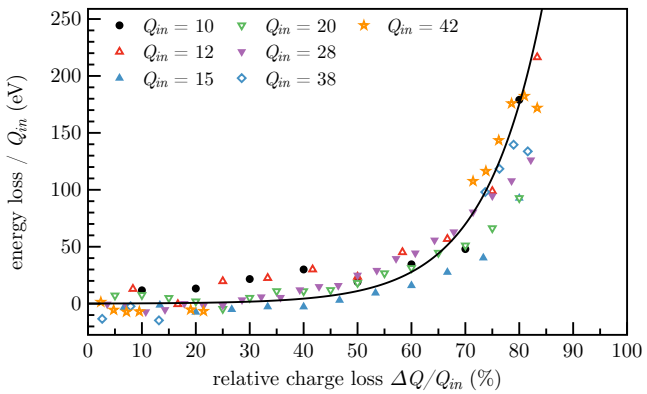

FIG. 6. (color online) Energy loss as function of relative charge loss $\Delta Q/Q_{in}$ for different incident charge states of Xe and also different incident kinetic energies of $E_{kin} = 4400\,\text{eV}\times Q_{in}$. The energy loss was rescaled by a factor Q_{in}^{-1} (see text), whereas now all energy losses follow a single exponential function. Negativ values are a result of limited measurement accuracy.

parameters are varied now. The data is shown in fig 6, where the measured energy loss is rescaled by a factor Q_{in}^{-1}. In fact, the rescaled energy losses follow all the same dependence on the (relative) charge exchange $\Delta Q/Q_{in}$.

IV. CONCLUSION

Electronic energy loss ΔE at low velocities is considered to be proportional to the ion velocity v

$$\Delta E(v, Q_{in} \approx 0) \propto v \tag{1}$$

which is in a narrow velocity range also observed in our measurements. However, we see a strong dependence on the incident and exit charge states,

$$\Delta E(v, Q_{in}, Q_{exit}) \propto v f(Q_{in}, Q_{exit}), \tag{2}$$

where $f(Q_{in}, Q_{exit})$ must be determined. In order to find $f(Q_{in}, Q_{exit})$ we showed that

$$\Delta E(v = const, Q_{in}, Q_{exit}) \propto \delta(Q_{exit}) Q_{in}^2 \text{ or} \tag{3}$$

$$\propto Q_{in} \mathrm{e}^{\gamma \frac{Q_{in}-Q_{exit}}{Q_{in}}} \tag{4}$$

(β and γ are constants, $\delta()$ is some function depending on Q_{exit}) and

$$\Delta E(v, \Delta Q/Q_{in}) \propto Q_{in} \mathrm{e}^{\gamma \frac{\Delta Q}{Q_{in}}}. \tag{5}$$

The velocity dependence is weak and the energy loss is dominated by charge exchange. The exponential dependence on charge exchange is found by comparing different data sets (see fig. 6) and finding a common fit function. Note that eq. (3) can easily be obtained from eq. (4) by a simple Taylor expansion. The universal form (5) contains implicitly the velocity dependence, because the energies used are $4400\,\mathrm{eV} \times Q_{in}$ and thus the velocities scale with $\sqrt{Q_{in}}$.

Additionally to the explicit velocity dependence discussed here, charge exchange may also depend on the ion velocity (i.e. $\Delta Q = \Delta Q(v)$). Charge exchange from resonant charge transfer $\Delta Q_{res}(v)$ depends strongly on the velocity, because it determines the time frame for charge transfer. Nonetheless, resonant charge transfer does not contribute to energy loss [26]. Non-resonant charge transfer $\Delta Q_{non-res}$ as in case of close ion-target approach and quasi-molecule formation [27, 28], on the other hand, may contribute to energy loss, whereas it does not depend on the ion velocity (in the velocity range discussed here). The bimodal exit charge state distribution in our measurements for carbon nanomembranes was attributed to different impact parameter regimes upon collisions from the angular dependence of the charge exchange [22]. Small charge exchange, associated with large target-projectile distances, may therefore only result from resonant charge transfer, i.e. here $\Delta Q = \Delta Q_{res}(v) \ll Q_{in}$. Large charge exchange on the contrary contains contributions from both resonant and non-resonant charge transfer, i.e. $\Delta Q = \Delta Q_{res}(v) + \Delta Q_{non-res} \lesssim Q_{in}$.

[1] N. Bohr, Philos. Mag. **25**, 10 (1913).
[2] H. Bethe, Ann. Phys. **397**, 325 (1930).
[3] F. Bloch, Ann. Phys. **16**, 285 (1933).
[4] J. Lindhard and M. Scharff, Phys. Rev. **124**, 128 (1961).
[5] P. Sigmund, Phys. Rev. A **54**, 3113 (1996).
[6] P. Sigmund, Phys. Rev. A **56**, 3781 (1997).
[7] P. Sigmund, *Mat. Meddelelser Udgivet Af Det K. Danske Vidensk. Selsk.*, Vol. 52 (2006) p. 557.
[8] H.-D. Betz, Rev. Mod. Phys. **44**, 465 (1972).
[9] R. Herrmann, C. L. Cocke, J. Ullrich, S. Hagmann, M. Stäckli, and H. Schmidt-Böcking, Phys. Rev. A **50**, 1435 (1994).
[10] S. Winecki, C. L. Cocke, D. Fry, and M. P. Stöckli, Phys. Rev. A **53**, 4228 (1996).
[11] M. Hattass, T. Schenkel, A. V. Hamza, A. V. Barnes, M. W. Newman, J. W. McDonald, T. R. Niedermayr, G. A. Machicoane, and D. H. Schneider, Phys. Rev. Lett. **82**, 4795 (1999).
[12] M. Imai, M. Sataka, K. Kawatsura, K. Takahiro, K. Komaki, H. Shibata, H. Sugai, and K. Nishio, Nucl. Instruments Methods Phys. Res. Sect. B Beam Interact. with Mater. Atoms **267**, 2675 (2009).
[13] E. Lamour, P. D. Fainstein, M. Galassi, C. Prigent, C. a. Ramirez, R. D. Rivarola, J.-P. Rozet, M. Trassinelli, and D. Vernhet, J. Phys. Conf. Ser. **635**, 032022 (2015).
[14] N. Bohr, Mat. Meddelelser Udgivet Af Det K. Danske Vidensk. Selsk. **18**, 1 (1948).
[15] T. Schenkel, M. A. Briere, A. V. Barnes, A. V. Hamza, K. Bethge, H. Schmidt-Böcking, and D. H. Schneider, Phys. Rev. Lett. **79**, 2030 (1997).
[16] F. Allegrini, R. W. Ebert, S. a. Fuselier, G. Nicolaou, P. Bedworth, S. Sinton, and K. J. Trattner, Opt. Eng. **53**, 024101 (2014).
[17] A. El-Said, R. Neumann, K. Schwartz, and C. Trautmann, Nucl. Instruments Methods Phys. Res. Sect. B Beam Interact. with Mater. Atoms **245**, 250 (2006).
[18] C. Lemell, A. El-Said, W. Meissl, I. Gebeshuber, C. Trautmann, M. Toulemonde, J. Burgdörfer, and F. Aumayr, Solid. State. Electron. **51**, 1398 (2007).
[19] A. S. El-Said, R. Heller, W. Meissl, R. Ritter, S. Facsko, C. Lemell, B. Solleder, I. C. Gebeshuber, G. Betz, M. Toulemonde, W. Möller, J. Burgdörfer, and F. Aumayr, Phys. Rev. Lett. **100**, 237601 (2008).
[20] R. A. Wilhelm and W. Möller, Phys. Rev. A **submitted** (2015).
[21] A. Turchanin and A. Gölzhäuser, Prog. Surf. Sci. **87**, 108 (2012).
[22] R. A. Wilhelm, E. Gruber, R. Ritter, R. Heller, S. Facsko, and F. Aumayr, Phys. Rev. Lett. **112**, 153201 (2014).
[23] O. B. Firsov, Sov Phys Jetp-Ussr **9**, 1076 (1959).
[24] F. F. Komarov and M. A. Kumakhov, Phys. Status Solidi **58**, 389 (1973).
[25] J. F. Ziegler, J. P. Biersack, and U. Littmark, *Vol. 1 - The Stopping and Range of Ions in Solids*, edited by J. Ziegler (Pergamon Press, New York, 1985).
[26] J. I. Juaristi, A. Arnau, P. M. Echenique, C. Auth, and H. Winter, Phys. Rev. Lett. **82**, 1048 (1999).

[27] N. Stolterfoht, A. Arnau, M. Grether, R. Köhrbrück, A. Spieler, R. Page, A. Saal, J. Thomaschewski, and J. Bleck-Neuhaus, Phys. Rev. A **52**, 445 (1995).

[28] A. Arnau, R. Köhrbrück, M. Grether, A. Spieler, and N. Stolterfoht, Phys. Rev. A **51**, R3399 (1995).